1-1-2010

Deep-ultraviolet photodetectors from epitaxially grown NixMg1-xO

J. W. Mares
University of Central Florida

R. C. Boutwell
University of Central Florida

M. Wei
University of Central Florida

A. Scheurer
University of Central Florida

W. V. Schoenfeld
University of Central Florida

Deep-ultraviolet photodetectors from epitaxially grown $Ni_xMg_{1-x}O$

Cite as: Appl. Phys. Lett. **97**, 161113 (2010); https://doi.org/10.1063/1.3503634
Submitted: 21 July 2010 . Accepted: 28 September 2010 . Published Online: 22 October 2010

J. W. Mares, R. C. Boutwell, M. Wei, A. Scheurer, and W. V. Schoenfeld

Deep-ultraviolet photodetectors from epitaxially grown $Ni_xMg_{1-x}O$

J. W. Mares,[a] R. C. Boutwell, M. Wei, A. Scheurer, and W. V. Schoenfeld
CREOL/The College of Optics and Photonics, University of Central Florida, 4000 Central Florida Blvd., Orlando, Florida 32816, USA

(Received 21 July 2010; accepted 28 September 2010; published online 22 October 2010)

Deep-ultraviolet (DUV) photodetectors were fabricated from high quality $Ni_xMg_{1-x}O$ epitaxially grown by plasma-assisted molecular beam epitaxy on an approximately lattice matched MgO ⟨100⟩ substrate. A mid-range Ni composition (x=0.54) $Ni_xMg_{1-x}O$ film was grown for DUV (λ_{peak} <300 nm) photoresponse and the film was characterized by reflected high-energy electron diffraction, Rutherford backscattering spectroscopy, x-ray diffraction, and optical transmission measurements. Photoconductive detectors were then fabricated by deposition of symmetric interdigitated contacts (10 nm Pt/150 nm Au) with contact separations of 5, 10, and 15 μm. The detectors exhibited peak responsivities in the DUV ($\lambda_{peak} \approx 250$ nm) as high as 12 mA/W, low dark currents ($I_{dark} < 25$ nA), and DUV:visible rejection ratio of approximately 800:1. © *2010 American Institute of Physics*. [doi:10.1063/1.3503634]

Various binary and ternary oxide semiconductors have been of growing interest recently as potential candidates for application in deep ultraviolet (DUV, $\lambda < 300$ nm) optoelectronic technologies. Semiconductors with direct band gaps greater than 4.35 eV find application in solar blind detection of radiation naturally attenuated by stratospheric ozone ($\lambda < 285$ nm). In medicine, the germicidal applications of ultraviolet-C light (UVC, $\lambda < 280$ nm) are well known and exploited as are its uses in the treatment of skin conditions such as psoriasis, eczema, and acne. Likewise, in manufacturing and industry DUV light is exploited in diverse applications such as photochemical processing, compound curing, and transistor erasure in erasable programmable read-only memory chips.

Here we present the epitaxial growth and characterization of approximately lattice matched epitaxial $Ni_xMg_{1-x}O$ on single-crystal ⟨100⟩ MgO for DUV photoconductors. This ternary compound is highly structurally compatible with the well exploited cubic $Zn_xMg_{1-x}O$ (Refs. 1 and 2) and has also already proven to be a useful optoelectronic material unto itself.[3,4] In complement to $Zn_xMg_{1-x}O$, which exhibits strong *n*-type propensity,[5–8] $Ni_xMg_{1-x}O$ exhibits a strong intrinsic *p*-type propensity and can also be *p*-doped extrinsically.[9–15] NiO and MgO are mutually miscible and the complete compositional range of $Ni_xMg_{1-x}O$ maintains a rocksalt cubic (B1) crystal structure with only $\varepsilon_{MgO}=0.8\%$ deviation in lattice constant ($a_{NiO}=4.177$ Å, $a_{MgO}=4.213$ Å).[16–18] Thus the ternary material is approximately lattice matched to commercially available MgO substrates. The band gap of NiO is approximately 3.6 eV (direct, $\lambda=344$ nm) and the ternary $Ni_xMg_{1-x}O$ exhibits band gap tunability across the 3.6–7.8 eV spectral region. Although prior efforts of NiMgO film growth and application have been conducted,[3,4,16–18] no literature exists on devices fabricated from molecular beam epitaxy (MBE) grown NiMgO thin films nor has there been any report of NiMgO growth on lattice matched single-crystal substrates.

In this research, epitaxial $Ni_xMg_{1-x}O$ was grown, characterized and exploited in DUV photoconductors. The film was grown as initially presented in Refs. 1 and 19, with subsequent refinements in growth parameters. In brief, the undoped (or unintentionally doped) film was grown with an MBE system, employing a radio-frequency oxygen plasma source. Elemental Mg and Ni (purity 99.99% and 99.9995%, respectively) were thermally evaporated from Knudsen cells. The film was grown on a single-crystal MgO ⟨100⟩-oriented 1 $in.^2$ substrate (MTI Crystal) with surface roughness measured to be less than ~5 Å. The substrate was cleaned in acetone, isopropanol, and de-ionized water ultrasonic baths then dried with N_2 flow. The substrate was degassed in a separate, vacuum-connected preparation chamber prior to growth. During growth O_2 flow rates ranged from 0.5 to 1.5 standard cubic centimeter per minute and substrate temperature was fixed at 700 °C. To improve surface quality for growth, a homoepitaxial MgO layer was first grown.

To assess film surface order *in situ*, reflection-high energy electron diffraction (RHEED) monitoring was carried out periodically during growth. Film composition and thickness were determined by Rutherford Backscattering (RBS) using 2.25 MeV He^{2+} particles and film thickness was confirmed by a Veeco Dektak 150 Profiler. X-ray diffraction (XRD) characterization was carried out with a Rigaku D/MAX x-ray diffractometer using Cu K_α radiation ($\lambda = 1.540\,56$ Å). Cataloged information about XRD spectra was obtained from JCPDS card numbers 045-0946 (MgO), 78-0643, and 89-7130 (NiO). Transmission spectrophotometry was carried out at room temperature using a Cary 500 UV-VIS spectrophotometer.

Photoconductive devices were then fabricated by standard photolithographic techniques. Conventional interdigitated contact patterns were designed with 5, 10, and 15 μm contact separations and a total device area of 1 mm^2. Contact metals were evaporated by an electron beam deposition system (Temescal FC-2000). Pt/Au contact metals (10 nm/150 nm) were chosen for Ohmic behavior to reduce or eliminate potential gain effects resulting from interfacial charge accumulation. Spectral responsivity measurements were conducted at room-temperature by illuminating the devices with a Xe lamp (300 W) passed through a monochromater while bias voltage and device current measurement were provided

[a]Electronic mail: jmares@mail.ucf.edu.

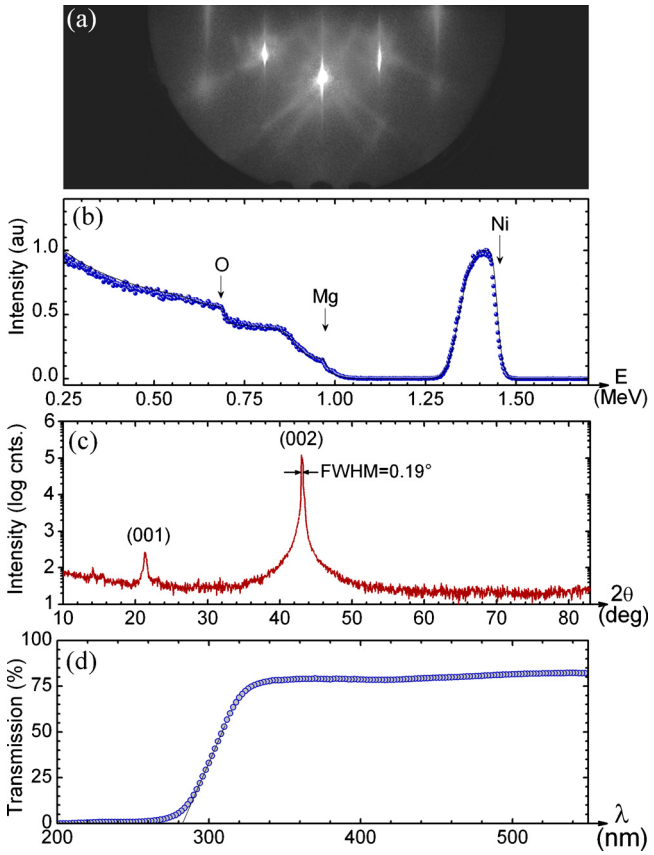

FIG. 1. (Color online) Characterizations of the $Ni_{0.54}Mg_{0.46}O$ film including (a) postgrowth RHEED indicating good surface order, (b) RBS spectrum of the film quantifying the composition, (c) XRD spectrum showing the highly oriented character of the film, and (d) optical transmission spectrum illustrating the UVC absorption edge.

by a Keithley 2400 source-meter. Because of the persistent photoconductivity exhibited by these devices, a typical lock-in amplification scheme is not applicable. Rather, light exposure was shuttered and illumination time was set to 3 s, which is greater than the time needed to saturate response. Responsivity values are corrected for both contact obscuration and approximate reflection loss as estimated by spectrophotometry presented herein and in prior works.[1,19]

Figure 1(a) shows the RHEED pattern of the $Ni_{0.54}Mg_{0.46}O$ film immediately after growth ([110] azimuth). Streakiness and relative brightness of the pattern implies good long range lateral surface order of the film. An RBS spectrum of the film is shown in Fig. 1(b) with the experimental data (symbols) overlaid by the modeled backscattered spectrum (solid). The Ni concentration was determined to be 54% (x=0.54) and the RBS spectrum indicates that the film is approximately 175 nm thick, as was confirmed by profilometry. In Fig. 1(c), the XRD spectrum illustrates the highly oriented nature of the $Ni_xMg_{1-x}O$ film as well as its cubic phase and (001) orientation. A standard θ-2θ scan was executed over the range $10° \leq 2\theta \leq 90°$. The only peaks observed for the film are attributed to the (001) and (002) lattice planes, of which the (002) was stronger by more than two orders of magnitude. The full-width half-maximum of the (002) peak was fitted to be 0.19°. The (111) diffraction peak would appear as the second most intense peak for randomly oriented polycrystalline NiO and would be located at $2\theta=36.939°$ for this stoichiometry. This peak's absence in

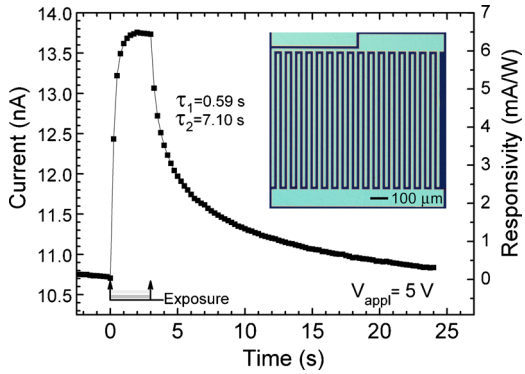

FIG. 2. (Color online) Photocurrent generated through the device (and corresponding responsivity) by 250 nm light. Inset shows the standard contact device geometry used.

the spectrum further demonstrates the oriented character of the film. Figure 1(d) shows the transmission of the film illustrating the abrupt DUV material band-edge absorption. A simple linear extension of the film's transmission edge to the λ-axis indicates a transmission cutoff wavelength of approximately 283 nm.

The $Ni_{0.54}Mg_{0.46}O$ devices were found to exhibit a persistent photoconductivity commensurate with that often observed in photoconductive devices.[20–22] Persistent photoconductivity was observed in these films by the authors previously and is found to be reduced with proper growth conditions (in general, higher substrates temperatures and reduced growth rates) and postgrowth treatment not discussed here. Figure 2 exemplifies this photocurrent persistence when a device (contact separation of 5 μm, $V_{applied}=5$ V) is illuminated by DUV light ($\lambda=250$ nm, $P_{incident} \approx 400$ nW) for 3 s. The induced photocurrent response saturates in fewer than 2 s of exposure. Upon ceasing illumination, measureable photocurrent persists for more than 20 s. The response decay is best fit by a two-term exponential form $[R(t)=A+Be^{-t/\tau 1}+Ce^{-t/\tau 2}]$. The faster of the two decay constants is likely associated with capacitive effects of the large-area devices, while the slower constant is attributed to presently unidentified deep-level defects shown to be associated with persistent photoconductivity. For the device shown the time constants are fitted to be $\tau_1=0.59$ s and $\tau_2=7.10$ s.

Device responsivities and dark currents were measured over the range of voltages which were found to promote stable, consistent device behavior. Maximum voltages were 10 V, 75 V, and 100 V for 5 μm, 10 μm, and 15 μm detector contact separations, respectively. Device peak responsivities as a function of applied voltage are plotted in Fig. 3(a). All devices were found to have approximately the same peak-response wavelength of 250 nm (the spectral resolution limits of measurement were $\Delta\lambda=5$ nm). The differential device responsivities (change in responsivity with respect to voltage) were found to be approximately 1.19 mA W^{-1} V^{-1}, 0.18 mA W^{-1} V^{-1}, and 0.016 mA W^{-1} V^{-1} for 5 μm, 10 μm, and 15 μm separations, respectively. The maximum observed responsivity was 12 mA/W measured in the 5-μm-separation device at an applied voltage of 10 V ($\lambda=250$ nm). Devices also exhibited linear I-V characteristics with low dark current, as illustrated in Fig. 3(b), with all measured dark currents less than approximately 25 nA. Device resistances were 0.45, 2.7, and 31 GΩ in order of increasing contact separation. Both responsivity and resistance

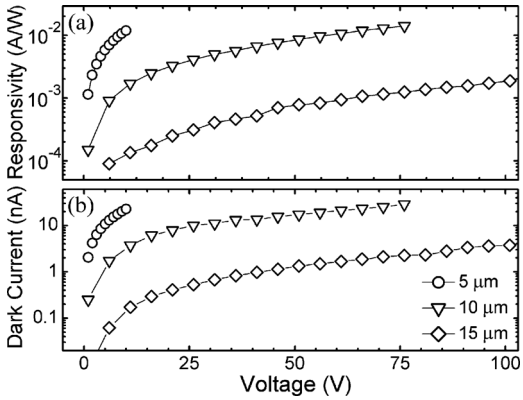

FIG. 3. (a) The voltage-dependent photoconductor responsivity at peak-response wavelength and (b) the corresponding device dark current.

values scaled approximately as expected by accounting for changes in contact separation and effective conduction channel length.[23] It should be noted that long carrier lifetimes are often associated with high device gain, sometimes leading to responsivities greater than unity quantum efficiency. However, the high resistance of these films—likely due to low carrier mobility observed in such ionic compounds—limits the gain of these devices. Interrogation of these compounds by Hall measurement is therefore an important continuation of this study.

Finally, the spectral response of the photoconductors is exemplified in Fig. 4. The device response spectrum (5 μm contact separation, $V_{applied}=10$ V) exhibits a clear response edge around 300 nm. As stated, the maximum responsivity is measured at $\lambda=250$ nm and is approximately 12 mA/W. The DUV:visible (DUV:VIS) rejection ratio ($R_{250\ nm}/R_{400\ nm}$) is found to be approximately 800:1.

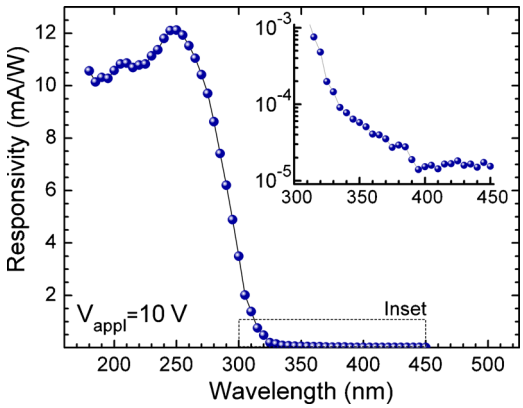

FIG. 4. (Color online) $Ni_xMg_{1-x}O$ photoconductor spectral responsivity. The devices exhibit abrupt UVC response-cutoff and a DUV:VIS rejection ratio of 800:1.

In summary, this work describes the growth and characterization of an epitaxial $Ni_{0.54}Mg_{0.46}O$ thin film on approximately lattice-matched MgO (100) and its subsequent application in photoconductive DUV detectors. Photoconductors with various contact separations (5, 10, and 15 μm) were fabricated by deposition of interdigitated Pt/Au contacts and characterized in terms of temporal response, spectral response, and voltage-dependence of responsivity and dark current. Distinct DUV responsivity ($\lambda_{peak}=250$ nm) with good visible rejection (800:1 selectivity) and high peak responsivity ($R_{max}=12$ mA/W) demonstrate the applicability of this ternary compound to DUV optoelectronic applications.

[1] J. W. Mares, R. C. Boutwell, M. T. Falanga, A. Scheurer, and W. V. Schoenfeld, Proceedings of MRS 2009 Fall Meeting (Mater. Res. Soc. Symp. Proc., Warrendale, 2009), Vol. 1201.
[2] H. F. Wong, K. H. Wong, and C. H. Lau, Phys. Status Solidi A **206**, 2202 (2009).
[3] Z. G. Ji, Z. P. He, K. Liu, S. C. Zhao, and Z. J. He, J. Cryst. Growth **273**, 446 (2005).
[4] Y. Zhao, J. Zhang, D. Jiang, C. Shan, Z. Zhang, B. Yao, D. Zhao, and D. Shen, J. Phys. D: Appl. Phys. **42**, 092007 (2009).
[5] N. B. Chen and C. H. Sui, Mater. Sci. Eng., B **126**, 16 (2006).
[6] S. Choopun, R. D. Vispute, W. Yang, R. P. Sharma, T. Venkatesan, and H. Shen, Appl. Phys. Lett. **80**, 1529 (2002).
[7] A. Ohtomo, M. Kawasaki, T. Koida, K. Masubuchi, H. Koinuma, Y. Sakurai, Y. Yoshida, T. Yasuda, and Y. Segawa, Appl. Phys. Lett. **72**, 2466 (1998).
[8] Z. G. Ju, C. X. Shan, D. Y. Jiang, J. Y. Zhang, B. Yao, D. X. Zhao, D. Z. Shen, and X. W. Fan, Appl. Phys. Lett. **93**, 173505 (2008).
[9] S. Lany, J. Osorio-Guillen, and A. Zunger, Phys. Rev. B **75**, 241203 (2007).
[10] U. S. Joshi, Y. Matsumoto, K. Itaka, M. Sumiya, and H. Koinuma, Appl. Surf. Sci. **252**, 2524 (2006).
[11] L. Ai, G. Fang, L. Yuan, N. Liu, M. Wang, C. Li, Q. Zhang, J. Li, and X. Zhao, Appl. Surf. Sci. **254**, 2401 (2008).
[12] Y. M. Lu, W. S. Hwang, J. S. Yang, and H. C. Chuang, Thin Solid Films **420–421**, 54 (2002).
[13] M. Eleruja, G. Egharevba, O. Abulude, O. Akinwunmi, C. Jeynes, and E. Ajayi, J. Mater. Sci. **42**, 2758 (2007).
[14] H. Ohta, M. Hirano, K. Nakahara, H. Maruta, T. Tanabe, M. Kamiya, T. Kamiya, and H. Hosono, Appl. Phys. Lett. **83**, 1029 (2003).
[15] A. M. Salem, M. Mokhtar, and G. A. El-Shobaky, Solid State Ionics **170**, 33 (2004).
[16] J. S. Choi, H. Y. Lee, and K. H. Kim, J. Phys. Chem. **77**, 2430 (1973).
[17] A. Kuzmin and N. Mironova, J. Phys.: Condens. Matter **10**, 7937 (1998).
[18] A. Kuzmin, N. Mironova, J. Purans, and A. Rodionov, J. Phys.: Condens. Matter **7**, 9357 (1995).
[19] J. W. Mares, R. C. Boutwell, A. Scheurer, M. Falanga, and W. V. Schoenfeld, Proc. SPIE **7603**, 76031B (2010).
[20] S. J. Chung, M. S. Jeong, O. H. Cha, C.-H. Hong, E. K. Suh, H. J. Lee, Y. S. Kim, and B. H. Kim, Appl. Phys. Lett. **76**, 1021 (2000).
[21] C. V. Reddy, K. Balakrishnan, H. Okumura, and S. Yoshida, Appl. Phys. Lett. **73**, 244 (1998).
[22] V. S. Vavilov, P. C. Euthymiou, and G. E. Zardas, Phys. Usp. **42**, 199 (1999).
[23] E. Rosencher and B. Vinter, *Optoelectronics* (Cambridge University Press, Cambridge, 2002).